# IMMUNOCYTOCHEMICAL LOCALIZATION OF OPSIN IN OUTER SEGMENTS AND GOLGI ZONES OF FROG PHOTORECEPTOR CELLS

## An Electron Microscope Analysis of Cross-Linked Albumin-Embedded Retinas

DAVID S. PAPERMASTER, BARBARA G. SCHNEIDER, MARK A. ZORN, and JEAN P. KRAEHENBUHL

From the Departments of Pathology and Cell Biology, Yale University School of Medicine, New Haven, Connecticut 06510, and the Institute of Biochemistry, University of Lausanne, Lausanne, Switzerland

ABSTRACT

Adult vertebrate retinal cells (rod and cones) continuously synthesize membrane proteins and transport them to the organelle specialized for photon capture, the outer segment. The cell structures involved in the synthesis of opsin have been identified by means of immunocytochemistry at the electron microscope level. Two indirect detection systems were used: (*a*) rabbit antibodies to frog opsin were localized with ferritin conjugated $F(ab')_2$ of sheep antibodies to rabbit $F(ab')_2$ and (*b*) sheep antibodies to cattle opsin were coupled to biotin and visualized by means of avidin-ferritin conjugates (AvF). The reagents were applied directly to the surface of thin sections of frog retinal tissues embedded in glutaraldehyde cross-linked bovine serum albumin (BSA). Specific binding of anti-opsin antibodies indicates that opsin is localized in the disks of rod outer segments (ROS), as expected, and in the Golgi zone of the rod cell inner segments. In addition, we observed quantitatively different labeling patterns of outer segments of rods and cones with each of the sera employed. These reactions may indicate immunological homology of rod and cone photopigments. Because these quantitative variations of labeling density extend along the entire length of the outer segment, they also serve to identify the cell which has shed its disks into adjacent pigment epithelial cell phagosomes.

KEY WORDS rhodopsin · membrane biosynthesis · Golgi zones · immunocytochemistry · retina · rods and cones

Biosynthesis of cellular membranes may proceed along membranous pathways proposed for secretion of enzymes. An early hypothesis of Palade (28) modified recently by Hirano et al. (18) postulates the addition of oriented membrane proteins to membranes which move from regions

 J. CELL BIOLOGY © The Rockefeller University Press · 0021-9525/78/0401-196 $1.00

of synthesis, the rough endoplasmic reticulum (RER)[1] and Golgi complex, to the appropriate subcellular site for function such as the plasma membrane. An alternative mechanism of direct ribosomal binding and protein synthesis in the Golgi complex has been proposed (13). Study of this process in most eukaryotic cells is hampered by the complexity of biological membranes. We have been assisted in elucidating some of the intermediate steps of membrane biosynthesis by analysis of photoreceptor cell membrane biogenesis in the retina because of the molecular simplicity of the rod outer segment (ROS) membrane (9, 31) and its continuous renewal in the adult vertebrate (16, 36). The light-sensitive membranes of vertebrate rod photoreceptors are arranged as closely packed disks enclosed in a plasma membrane to form the outer segment. Cone outer segments (COS) are homologous arrays of invaginated lamellae of the plasma membrane (7). We recently reported evidence that newly synthesized frog opsin and a large intrinsic membrane protein are transported on readily sedimented membranes before their assembly into the disks of ROS (29, 30).

We have initiated immunocytochemical studies to define some of the cellular structures responsible for biosynthesis and transport of opsin to the outer segment. This report describes our initial results with the thin-sectioning technique of McLean and Singer (26) as modified by Kraehenbuhl and Jamieson (21) which employs aldehyde-fixed tissues embedded in glutaraldehyde cross-linked bovine serum albumin (BSA). We have localized opsin in the outer segment, as expected, and also in the Golgi area. These results, together with previous biosynthetic studies (7, 8, 16, 27, 33), suggest that the Golgi complex may contain newly synthesized opsin.

## MATERIALS AND METHODS

### *Preparation of Antibodies*

Rabbits were immunized with frog opsin contained in a strip of polyacrylamide gel after sodium dodecyl sulfate (SDS)-polyacrylamide gel electrophoresis as described previously (29, 30). A sheep was similarly immunized with cattle opsin. Antibodies were assayed for specificity by the two-dimensional immunoelectrophoretic technique of Converse and Papermaster (11). Cattle opsin affinity immunoabsorbents were prepared as described previously (30) or by the following modification: Opsin was electrophoretically eluted from the SDS gel and coupled to agarose-multichain poly-D,L-alanine-poly-L-lysine (PAL Agarose, Miles-Yeda, Israel) by reaction with 1-ethyl-3-(3-dimethyl-aminopropyl) carbodiimide-HCl (EDAC, Bio-Rad Laboratories, Richmond, Calif.). Anti-opsin sera from rabbits and the sheep were digested with pepsin at pH 4.5 to produce $F(ab')_2$ fragments, incubated with the immunoabsorbent at pH 7.4, and bound specific antibody fragments were eluted with 3 M KSCN (22). The specific antibody fragments were chromatographed on Sephadex G-150, 1.5 × 90 cm, in phosphate-buffered saline (0.15 M NaCl, 0.005 M $PO_4$, pH 7.4, 0.002 M $NaN_3$) to eliminate aggregates, concentrated by ultrafiltration to 1 mg/ml (Amicon PM30 filter, Amicon Corp., Scientific Sys. Div., Lexington, Mass.), and mixed with BSA to a concentration of 1%. Yields of specific antibody were determined by calculation of the protein content of specifically eluted antibody fragments, using an $E^{1\%}_{280\,nm} = 13.5$. Before use, all sera were centrifuged at 234,000 $g_{avg}$ (50,000 rpm, SW50.1 rotor, Beckman Instruments, Inc., Fullerton, Calif.) for 2 h.

### *BSA Embedding of Retinas and Immunocytochemical Reactions*

Light-adapted frogs (*Rana pipiens*) were decapitated 3–4 h after sunrise and the eyes were removed and fixed in 4% formaldehyde in 0.1 M phosphate buffer, pH 7.4. After 10 min, the anterior third of the eye cup was removed. After 2 h in the 4% formaldehyde, the tissue was fixed for 2 additional h in 4% formaldehyde and 2% glutaraldehyde in phosphate buffer at room temperature. The tissue was cut into 1-mm wide strips, which were washed for 1 h at 4°C in phosphate buffer. The tissue strips were incubated overnight in 30% BSA at 4°C in phosphate buffer, then transferred to a dialysis membrane for dehydration and embedding by fixation in 0.5% glutaraldehyde (22). Thin sections were obtained on carbon- and Formvar-coated grids. Reactions on the sectioned tissues with rabbit anti-frog opsin $F(ab')_2$ were detected with ferritin conjugated $F(ab')_2$ of sheep anti-rabbit $F(ab')_2$ prepared by the solid-phase conjugation procedure of Kraehenbuhl et al. (23). Biotin $F(ab')_2$ of sheep anti-cattle opsin and of nonimmune serum were prepared by reaction with biotin *N*-hydroxysuccinimide ester and detected by reaction with the avidin-ferritin conjugate (AvF) by the procedure of Heitzmann and Richards (17). Biotin *N*-hydroxysuccinimide ester and AvF were the kind gifts of Drs. Bonnie Wallace and Fred Richards (Yale University, New Haven, Conn.). Immediately before use, ferritin conjugates were centrifuged at 10,000 rpm for 2 min (Beckman microfuge, Beckman Instruments, Inc., Spinco Div., Palo Alto,

[1] *Abbreviations used in this paper:* AvF, avidin-ferritin conjugate; BSA, bovine serum albumin; COS, cone outer segment; PE, pigment epithelium; RER, rough endoplasmic reticulum; ROS, rod outer segment; SDS, sodium dodecyl sulfate.

Calif.) at 4°C. After reaction with the ferritin-conjugated second step reagents, the sections were washed thoroughly with buffer and stained successively with bismuth subnitrate, 1.2 mM, for 30 min (1), saturated uranyl acetate in 50% ethanol for 2 min/lead citrate, 80 mM, 2 min, dried, and viewed with a Philips 300 or 400 electron microscope at 80 KV. For comparison, some tissue blocks were dehydrated, Epon-embedded, and thin sectioned.

### *Quantitative Estimation of Antibody Labeling*

Outer segments of the different photoreceptors were labeled in a reproducible but different pattern by each of the three sera tested. Accordingly, labeling density was assessed by morphometric techniques described by Weibel et al. (34, 35). Mean ferritin grain counts/$\mu m^2$ (± SEM) were calculated and illustrate the quantitative variation in these labeling patterns (Table I). Since the inner segments were labeled to a much lesser extent, specific localization to the region of the Golgi complex was established by comparison of labeling by immune and nonimmune sera. Low magnification micrographs were prepared by one of us of all suitable inner segment regions which contained nuclei and relatively translucent areas which might represent Golgi complexes. Higher magnification micrographs of these areas were then prepared which contained no outer segments in the field. They were assigned a random number and given to two of us who had no knowledge of which ferritin-conjugated reagent was used in each case. Photomicrographs were scored independently for presence or absence of Golgi zones and labeling by ferritin-conjugated reagent. The results were then decoded and matched for concurrence of scoring, and the proportions of reactive Golgi complexes were calculated.

## RESULTS

### *Fine Structure of Photoreceptors*

The fine structure of photoreceptor cells investigated by electron microscopy of plastic-embedded retinas has been extensively reviewed (10). To compare BSA-embedded retina, we have illustrated the different photoreceptors of frog retina embedded in Epon (Fig. 1). Two classes of rod cells have been distinguished: red and green. The latter cell is characterized by a shorter ROS length, long and slender inner segment, cylindrical shape of the ROS, and the transmission of a green color when viewed end-on over white light. Single cones and principal cones have COS and an oil droplet juxtaposed at the apex of the inner segment near the clustered mitochondria. Accessory cones (a minor population) do not have oil droplets. Further details are summarized in Fig. 1. Horizontal cross sections of ROS reveal deep clefts termed incisures which divide the disks into multiple lobes. These incisures remain superimposed in complete alignment over the entire length of the ROS.

### *Structural Preservation of Retina Embedded in Cross-Linked BSA*

Subcellular structure is readily recognized in sections of BSA-embedded retina. Negatively stained ROS disk membranes, plasma membranes and incisures are seen in the outer segment (Fig. 2). Off-center longitudinal sections

TABLE I

*Outer Segment Ferritin Labeling Density by Antiserum to Frog and Cattle Opsin*

| | Ferritin molecules/$\mu m^2$ ± SEM | | | |
|---|---|---|---|---|
| | Red ROS | Green ROS | COS | PE |
| Anti-frog opsin | | | | |
| Serum no. 1 | 715 ± 25 (14)* | 647 ± 18 (12) | 336 ± 26 (24) | 40 ± 4 |
| Serum no. 2 | 461 ± 45 (11) | 303 ± 45 (6) | 97 ± 11 (9)‡<br>22 ± 5 (5) | 13 ± 2 |
| Anti-cattle opsin, biotin-labeled | 593 ± 20 (24) | 157 ± 11 (23) | 16 ± 3 (18) | 21 ± 3 |
| Nonimmune sera | | | | |
| $F(ab')_2$ | 34 ± 3 (6) | 43 ± 8 (4) | 21 ± 4 (5) | 23 ± 3 |
| Biotin-labeled $F(ab')_2$ | 4 ± 2 (9) | 4 ± 1 (10) | 3 ± 1 (15) | 15 ± 3 |

* Values in parentheses indicate the number of outer segments counted (see Figs. 3 and 5).

‡ Most of the cone areas were labeled at density above background while the others did not differ from background significantly (see Fig. 6).

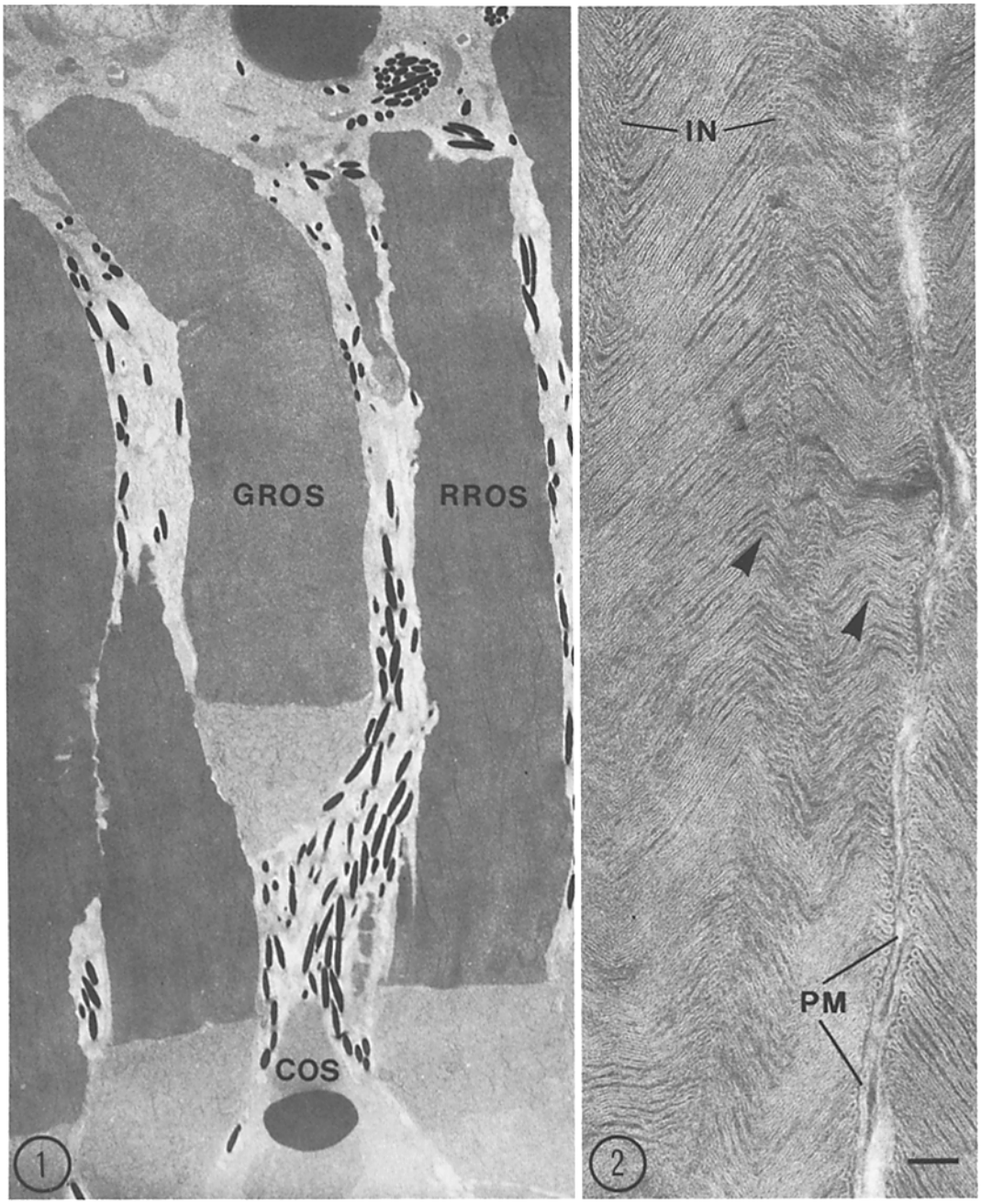


FIGURE 1 Low magnification electron micrograph of longitudinally sectioned retina embedded in Epon; red rods have long cylindrical outer segments (red ROS [*RROS*]) whereas green rods have shorter outer segments (green ROS [*GROS*]) and long tapered inner segments. Single and principal cones have COS adjacent to a large oil droplet in the inner segment. × 3,300. Compare Fig. 7.

FIGURE 2 ROS embedded in cross-linked BSA, thin sectioned and negatively stained by bismuth subnitrate, lead citrate, and uranyl acetate. Membranes of the ROS disk and plasma membrane (*PM*) appear unstained against a background of positively stained cytoplasm and intercellular space. During processing, disks become buckled and convoluted which generates a herringbone appearance in longitudinal section (arrows) and variation of plane of section within a single ROS. Incisures (*IN*) appear as abutting hairpin loops forming a dense line in the interior of the ROS. All subsequent illustrations are of frog retinas, embedded in cross-linked BSA and stained as described in Materials and Methods. Bar, 0.1 $\mu$m. × 70,000.

reveal these incisures as a linearly repeated duplication of the disk margin resembling small hairpin loops. The increased electron density of the interdisk space and intradisk space after staining with lead and uranyl salts may indicate the presence of other cytoplasmic components in this organelle which are not identified in the SDS-polyacrylamide gels of isolated membranes. The intercellular matrix and cell processes of pigment epithelial (PE) cells are less intensely stained (Figs. 1–7).

In the apical regions of the inner segment, pale-staining mitochondria are visualized as a tight cluster between the negatively stained RER membranes and the ROS (Figs. 3 and 6). The large oil droplet characteristic of frog single and principal cones near the junction of the inner and outer segment is not well stabilized during this procedure, and most of it usually is lost during recovery of the section (Figs. 5 and 6). Phagosomes filled with disks in pigment epithelial cells are well demarcated from the surrounding cell cytoplasm and the tips of nearby ROS (Figs. 8 and 9). Melanosomes of PE cells are usually displaced slightly or completely during the sectioning and may leave a residual empty vacuole (Fig. 9). The nucleus and its membrane are well defined (Figs. 10 and 11).

The pale-staining, longitudinally oriented structures near RER membranes and the nucleus (Figs. 10 and 11) resemble the Golgi complex of pancreatic cells studied with this technique (23) and are appropriately shaped for this cell (8, 16). In several sections of the inner segment, ovoid, relatively translucent structures ~0.1 $\mu$m in diameter are noted and may represent tubular or vesicular structures seen in Epon sections. They are especially prominent near the base of the outer segment and the Golgi complex (Figs. 3 and 10). They may represent negatively stained membranes tangentially sectioned that originated from smooth membrane channels or vesicles in the cytoplasm.

The technique of embedding in BSA necessarily involves considerable dehydration to form a hard block for thin sectioning. This may account for the distortion of disk orientation which results in a "herringbone" pattern between the aligned incisures (Fig. 2) and the small intermitochondrial cytoplasmic space (Fig. 3).

SPECIFICITY OF ANTISERA: The anti-frog opsin sera were tested extensively in our prior biosynthetic studies of opsin by the two-dimensional electrophoretic technique of Converse and Papermaster (11). Each antiserum reacted only with opsin migrating in the appropriate region of the gel. When frog retinal membranes were labeled with [$^{14}$C]leucine during in vivo incorporation and the isolated membranes were electrophoresed against each antiserum, newly synthesized opsin of the many newly synthesized proteins was the only protein immunoprecipitated. The data were presented in a prior report (29). The sheep anti-cattle opsin was tested similarly and reacted with frog and cattle opsin comparably, i.e. peak heights were similar. However, the sheep antiserum reaction formed a wider arc with either frog or cattle opsin than with the rabbit anti-frog opsin despite attempts to increase serum concentration to correct for the effect of a weaker antibody response in the sheep (average 0.2 mg/ml; range 0.1–0.8 mg/ml in various bleedings).

## IMMUNOCYTOCHEMICAL LOCALIZATIONS

(a) ROD OUTER SEGMENTS: Rather dense, specific labeling of frog ROS occurs with antibody to opsin (Figs. 3–7 and Table I). Intercellular processes of pigment epithelium (PE) and cell bodies of PE cells are unlabeled (Figs. 4, 5, and 8 and Table I). Moreover, the phagosomes of PE cells which contain fragments of ROS are also labeled (Figs. 8 and 9). On favorably oriented sections, the disk lamellae may be seen beneath the ferritin grains (Figs. 6–8). Occasionally, the ferritin is aligned along the disk (Fig. 6, *inset*). Usually, however, there is no obvious linear pattern in the binding of the ferritin-labeled complexes on ROS, perhaps because of the slightly tangential planes of section caused by the distorted disk structure. Along the ROS plasma membrane, bound antibody forms a line in some regions (Fig. 7, *inset*). Bound antibody-ferritin detecting rabbit anti-frog opsin is largely distributed in a dispersed pattern of individual molecules or in small clusters of two or three ferritin grains. Occasional dense clusters of 5–10 grains are scattered throughout the length of the ROS (Figs. 3–5 and 8). Aggregates were largely eliminated in both ferritin reagents by centrifugation and chromatography. Some of the large clusters occur in regions of slightly greater electron density in the tissue and may represent binding to tangentially sheared membranes which exposed antigen more favorably for reaction (Figs. 4 and 5).

While both red and green ROS are comparably labeled by one of the rabbit anti-frog opsin sera, the green ROS bind the other anti-opsin sera with a lower density (Table I). The sheep anti-cattle

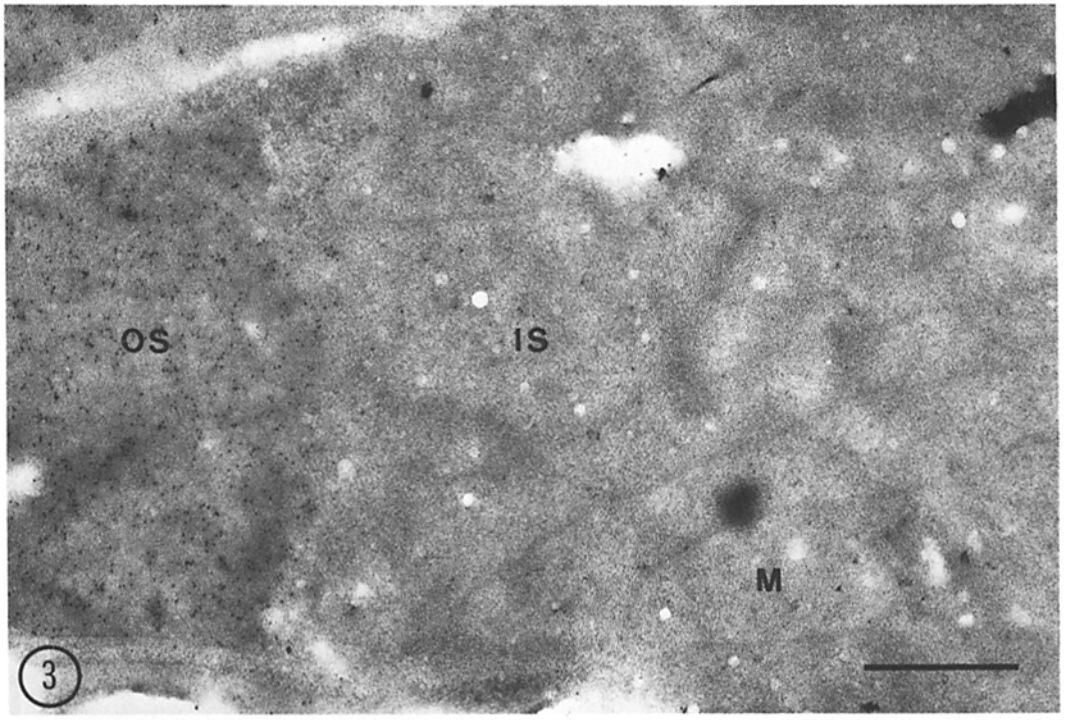


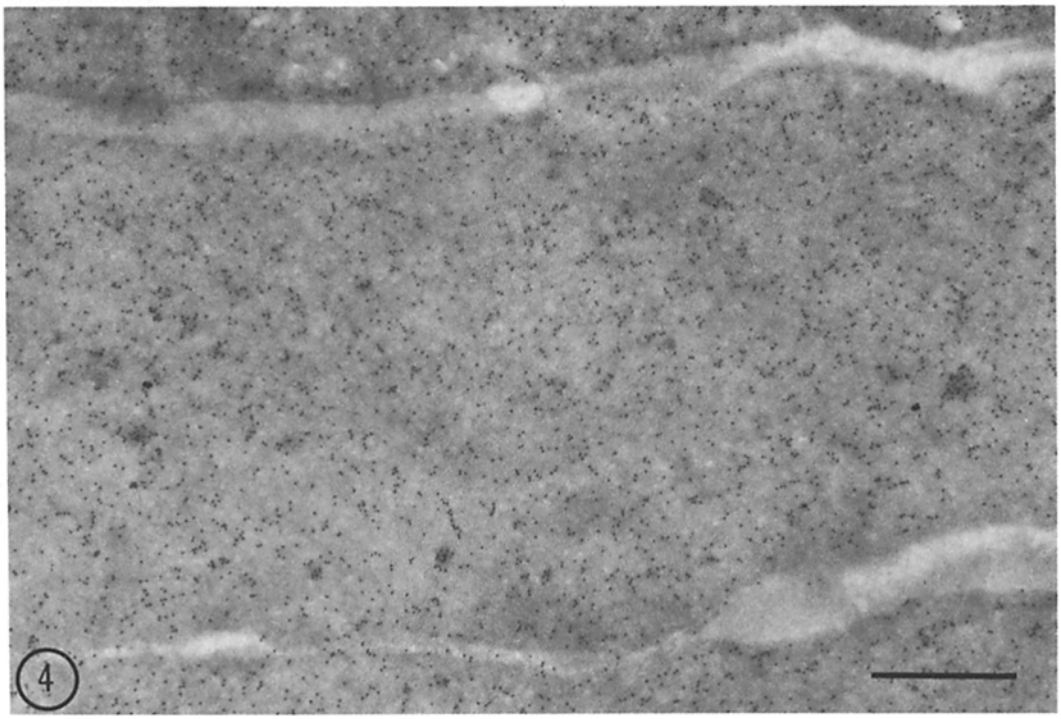


FIGURE 3 Junction between inner and outer segments (*OS*) of rod cells reacted with rabbit anti-frog opsin. Figs. 3–6, 8, and 10 are reacted with $F(ab')_2$ of rabbit anti-opsin, and the reactions are detected with ferritin-$F(ab')_2$ of sheep anti-rabbit $F(ab')_2$. In subsequent figures, "antibody" refers to the $F(ab')_2$ fragments. Localization of ferritin grains indicates the binding of anti-opsin. Occasional ferritin grains are noted below the junction of the OS and inner segment (*IS*) which is densely packed with negatively stained mitochondria (*M*). Abundant oval structures are scattered in the mitochondrial region and may represent sectioned tubular or vesicular components in the cytoplasm. Bar, 0.5 $\mu$m. × 40,000.

FIGURE 4 ROS labeled with anti-frog opsin serum no. 1. Dispersed single grains and small clusters of two to four ferritin grains predominate over red ROS (this figure) and green ROS which are labeled comparably by this serum (see Table I). Occasional clusters of five to ten grains appear in regions of slightly greater electron density. The absence of antibody binding to the intercellular space between the rods is an indication of the specificity of the reaction. Bar, 0.5 $\mu$m. × 38,000.

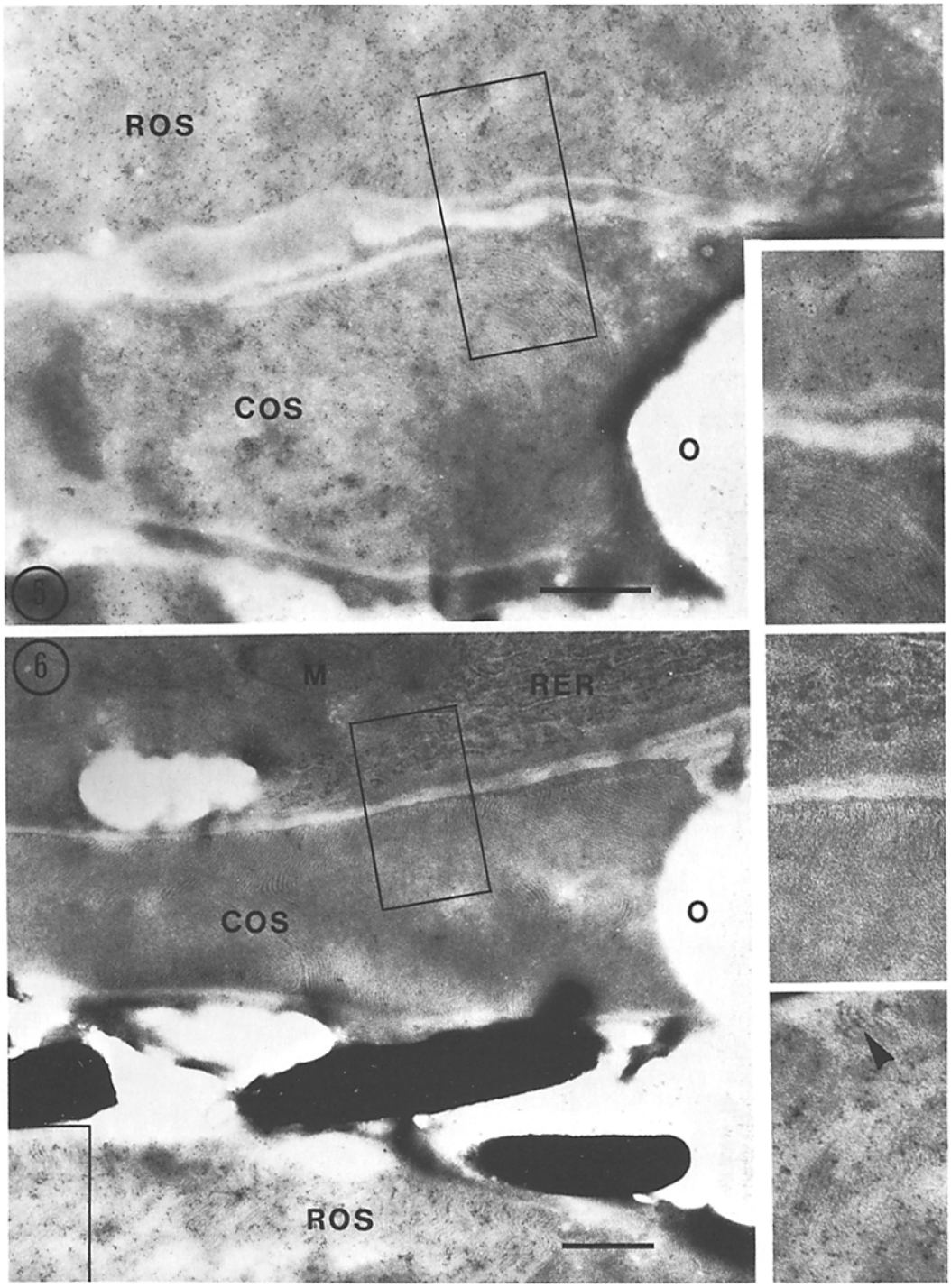


FIGURE 5 Reaction of rabbit anti-opsin serum no. 1 with COS. The cone cell is identified by its conical outer segment and the large oil droplet (*O*) in its inner segment. The labeling density on COS is about half of the density on adjacent red ROS. Bar, 0.5 μm. × 32,000. *Inset:* High magnification of the indicated area. × 46,000.

FIGURE 6 Absence of specific labeling of a COS with anti-frog opsin serum no. 2 (compare to Fig. 5). The labeling density of the adjacent ROS is comparable to that obtained with anti-frog opsin no. 1. Mitochondria, *M*. Bar, 0.5 μm. × 26,000. *Insets:* High magnification of indicated areas illustrates the relative degree of ferritin labeling. Arrow shows alignment of ferritin on the disk membrane. × 49,000.

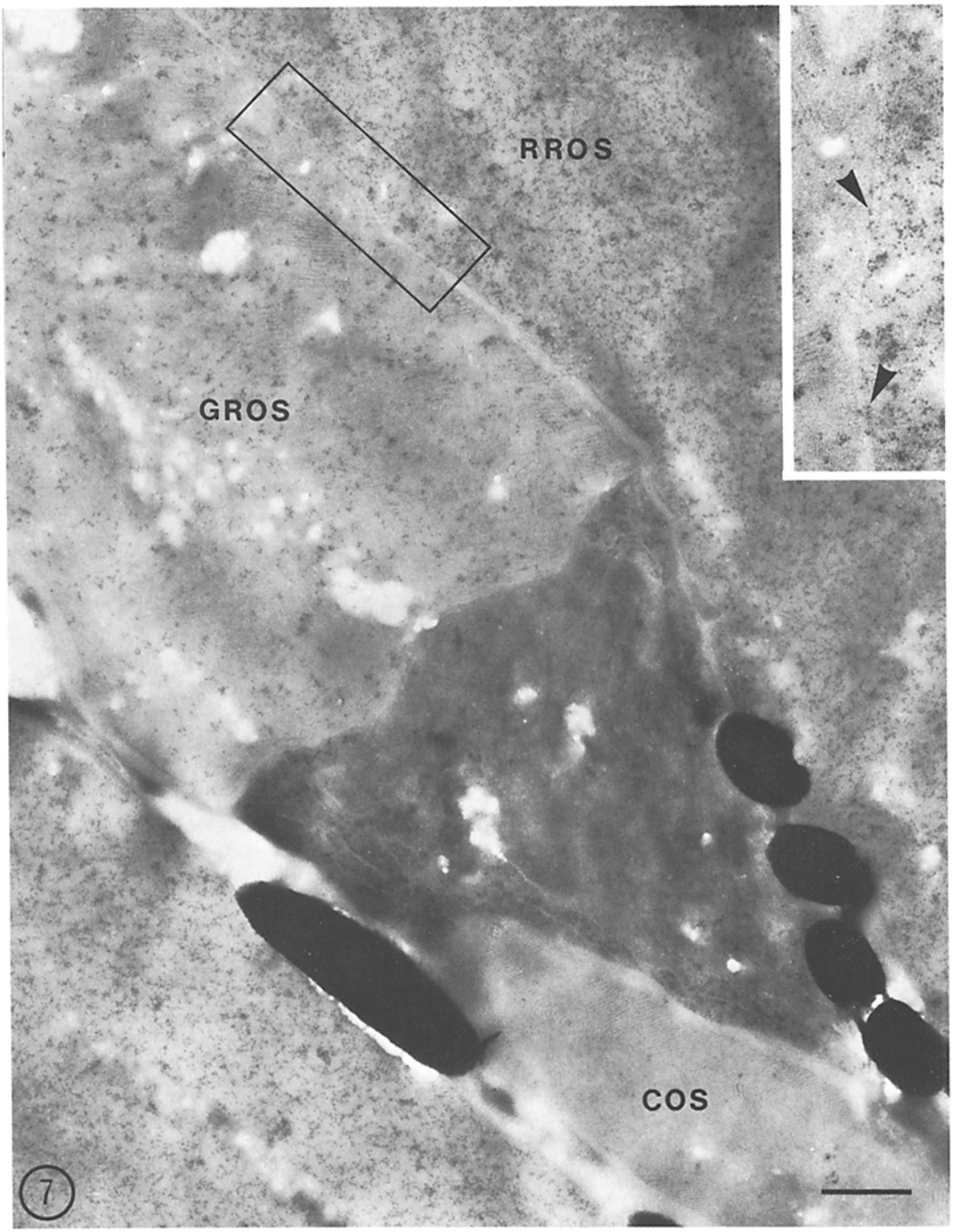


FIGURE 7 Biotin-labeled F(ab')$_2$ of sheep anti-cattle opsin serum reacts with frog red ROS (*RROS*) and green ROS (*GROS*) but not with COS. The bound antibody is detected with avidin-ferritin and is distributed in a dense, dispersed pattern of binding of single molecules on RROS with occasional large clusters of ferritin. The reduced density of labeling of GROS distinguishes the two rod cell types. Bar, 0.5 $\mu$m. × 26,000. *Inset:* The RROS plasma membrane and the GROS plasma membrane are also labeled linearly, suggesting the presence of opsin in the plasma membrane as well as the disk membranes of ROS. × 45,000.

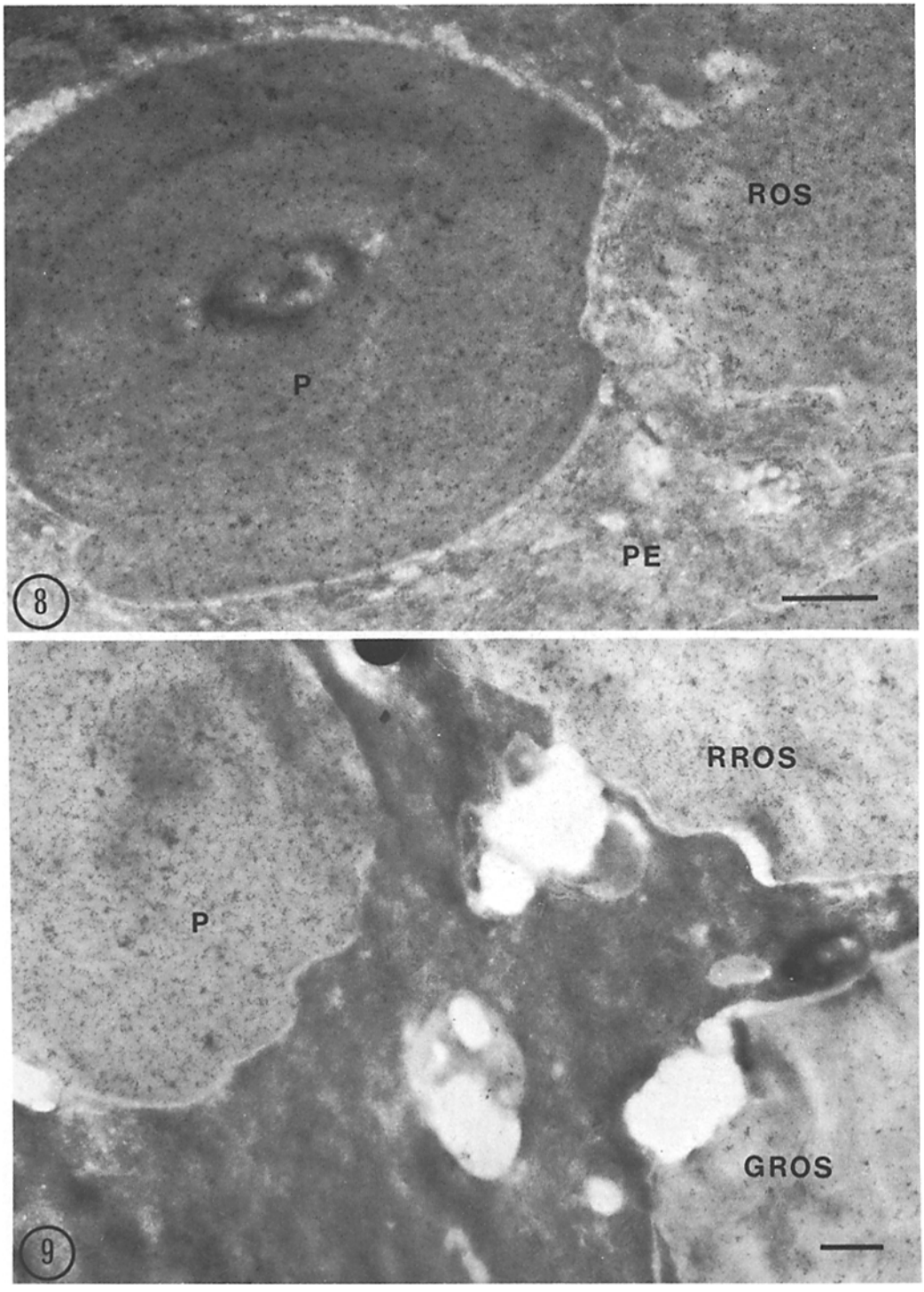


FIGURE 8 Phagosome (*P*) in the PE cell contains the shed disks of the adjacent ROS. Anti-frog opsin reacts with the ROS and the opsin persisting in the ingested disks of the phagosome. PE cell cytoplasm is nearly free of ferritin. Bar, 0.5 $\mu$m. × 28,000.

FIGURE 9 Phagosome of the PE cell contains disks from a frog red ROS (*RROS*) as indicated by its reaction with biotin-labeled anti-cattle opsin which binds to RROS in a dense labeling pattern (see Fig. 7 and Table I). The adjacent green ROS (*GROS*) is less densely labeled. Bound biotin-antibodies are detected with avidin-ferritin. Bar, 0.5 $\mu$m. × 18,000.

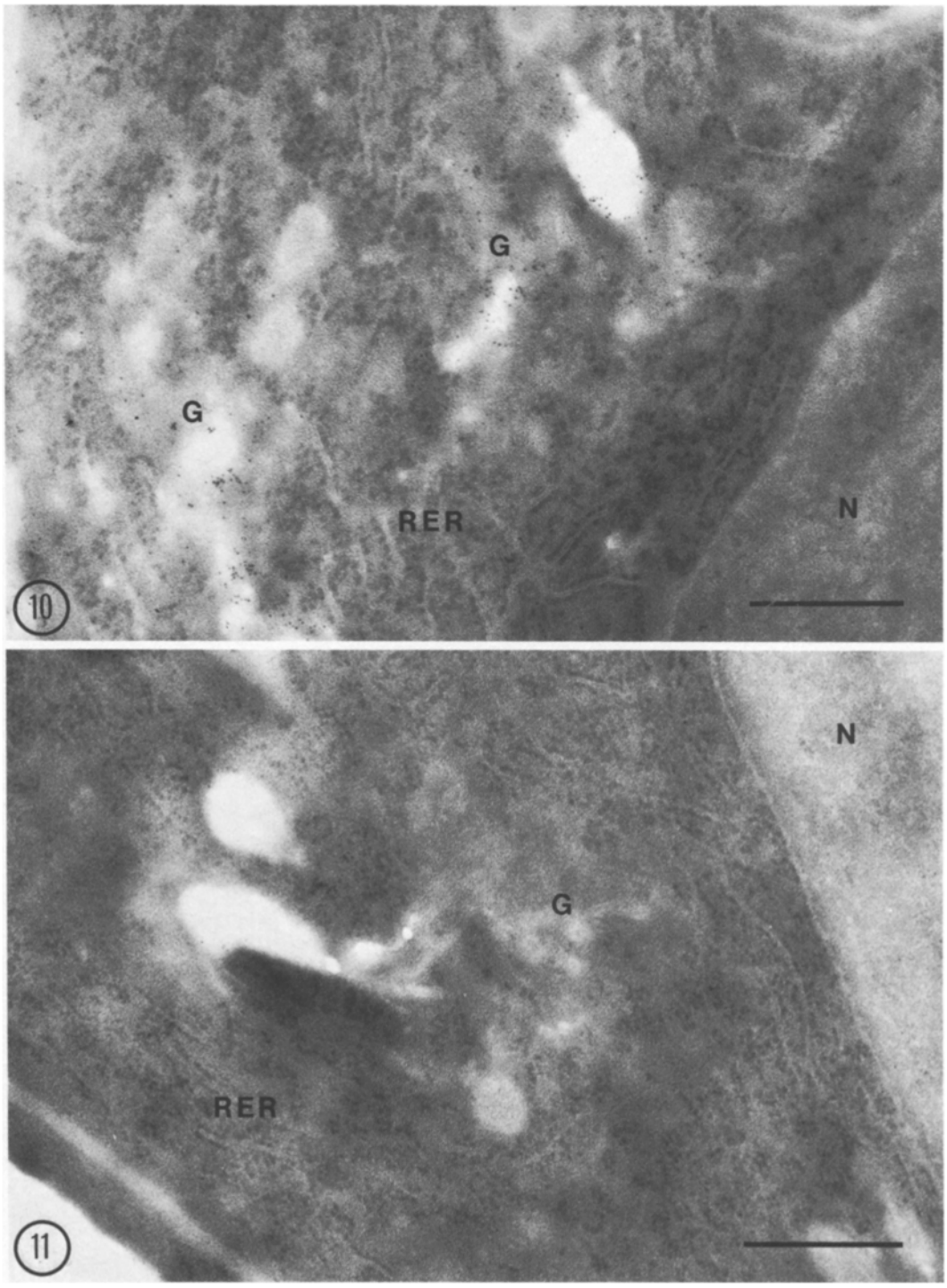


FIGURE 10 Reaction of anti-frog opsin with inner segment organelles. A pale-staining structure near the nucleus (*N*) lies next to negatively stained profiles of RER outlined by densely stained ribosomes. This probably represents the Golgi zone (*G*) of this cell. Ferritin grains are bound to this structure, especially at its borders. Bar, 0.5 $\mu$m. × 45,000.

FIGURE 11 Control section of rod inner segment near the nucleus (*N*) reacted with unimmunized rabbit serum IgG F(ab')$_2$. This section was chosen to illustrate the usual levels of nonspecific binding of F(ab')$_2$ to inner segment structures. Although occasional ferritin grains are seen near the probable Golgi zone (*G*), they are also scattered in low density over the nucleus and adjacent RER (Table II). There is considerably less staining of the Golgi zone in this section compared to the previous figure reacted with anti-opsin. Bar, 0.5 $\mu$m. × 46,000.

opsin labeled green ROS with ~25% of the labeling density of red ROS (compare Figs. 3–5 with Figs. 7 and 9). Red ROS were comparably labeled by rabbit anti-frog opsin and sheep anti-cattle opsin; this indicates that AvF provided comparable sensitivity of detection of bound first-stage antibodies when compared in this technique to detection with ferritin-antibody conjugates. Both ferritin-conjugated reagents were equally specific since background areas between cells and in PE cell cytoplasm were virtually free of label (Table I). Both ferritin labels were distributed as clusters and dispersed grains on red and green ROS. Since green ROS could react readily with one anti-frog opsin sera, the lower labeling densities with the other anti-frog opsin and anti-cattle opsin sera were not the result of variation in the physical properties of the sectioned surfaces of the two ROS regions.

The difference in labeling density of red ROS and green ROS extends along the entire length of the ROS. This difference could be used to indicate whether a group of disks within a PE cell phagosome were shed from the red ROS next to it or from an adjacent green ROS (Fig. 9). These reactions of sheep anti-cattle opsin upon sections of frog retina also indicate considerable antigenic cross-reactivity of frog red ROS opsin and cattle opsin, which confirms previous observations made with two-dimensional immunoelectrophoresis (11, 29). Anti-frog opsin serum no. 1 was also purified by affinity chromatography on a cattle opsin immunoabsorbent. Therefore the reaction of this antiserum equally with red and green ROS suggests that some antigenic determinants exist in common to all three opsins, i.e. frog red ROS and green ROS and cattle opsins are each reactive with the rabbit anti-frog opsin.

(b) CONE OUTER SEGMENTS: One rabbit (no. 1) immunized with frog opsin formed antibodies which labeled red and green ROS and also COS but with a lower and more variable labeling density of COS (Table I and Fig. 5). Another rabbit (no. 2) immunized the same day with the same antigenic preparations formed antibodies reactive with red and green ROS and some but not all COS (Fig. 6). About 35% of COS areas were unlabeled by this second rabbit anti-frog opsin serum. The level of ferritin binding over these unlabeled COS resembles adjacent areas of PE cell processes which are notably free of bound ferritin. This indicates that the binding of antibodies from these rabbits is specific, not a physical property of the multilamellar membranes of outer segments. The anti-cattle opsin serum does not react with COS despite its reactions with red and green ROS described above (Fig. 7 and Table I).

(c) INNER SEGMENTS: Sections of rod photoreceptor cell inner segments are reproducibly labeled by all three anti-opsin antibodies. A specific and prominent labeling density is associated with the translucent regions near the nucleus whose appearance is consistent with Golgi complexes (Figs. 10 and 11 and Table II). The Golgi complexes were unlabeled by unimmunized sera (0% false positive reactions) and were labeled in 24 of 52 Golgi zones stained with specific anti-opsin sera. Current limitations of the staining of tissues embedded in BSA for the visualization of membrane do not allow correlation between ferritin grains and underlying membranes in the RER and mitochondrial regions.

(d) CONTROLS: The primary control reaction is the absence of the labeling of ROS or inner segment regions when unimmunized antibody fragments are used as the first-stage reagent (Fig. 11 and Table II). In addition, both second-stage reagents, ferritin-conjugated goat anti-rabbit $F(ab')_2$ and AvF, do not bind in the absence of the specific first-stage reagent. Thus, nonspecific binding of these proteins does not occur to a sufficient degree in BSA-embedded retina to ob-

TABLE II

*Inner Segment Ferritin Labeling Density*

| | Ferritin molecules/$\mu m^2$ ± SEM | | | |
|---|---|---|---|---|
| | Golgi | RER | Mitochondria | Nucleus |
| Rabbit anti-opsin (1 + 2) | 57 ± 13 (12)* | 21 ± 4 (11) | 31 ± 7 (7) | 11 ± 4 (10) |
| | $P = 0.026$ | NS | NS | NS |
| Nonimmune rabbit serum | 9 ± 7 (6) | 12 ± 4 (6) | 21 ± 5 (6) | 14 ± 3 (7) |

$P$ was determined using the Student's $t$ test comparing the combined means of both anti-opsin and nonimmune sera.
* Values in parentheses indicate the number of cells counted.

scure low-density labeling reactions such as the reactions of COS and green ROS with antibodies to frog and cattle opsins, respectively (Figs. 5 and 7), and the specific labeling of Golgi complexes (Fig. 10 and Table II).

More important, adjacent cellular areas on sections stained with specific anti-opsin sera and the second-stage reagents are also notably free of bound ferritin. PE cell cytoplasm is virtually unstained except in phagosomes containing shed ROS disks (Fig. 8 and Table I). Also, most COS are unlabeled with two of our three antisera and illustrate the remarkable absence of nonspecific binding in the presence of antibody excess. After 1,000- to 10,000-fold dilution, labeling density was greatly reduced but the distribution was unchanged. These reactions with diluted anti-opsin sera are discussed in greater detail in a related paper.[2]

## DISCUSSION

While the detection of cell surface antigens by immunocytochemical techniques has a long history, the ability to localize intracellular antigens *in situ* by high resolution techniques has been inhibited by the impermeability of the cell membranes to antibodies and antibody fragments. The development of direct labeling of sections of tissue embedded in a hydrophilic matrix of cross-linked BSA provides a new approach to localization which does not depend upon further manipulation of the section to expose antigens and restricts protein perturbation to aldehyde treatment and dehydration (21, 26). We wished to examine the BSA-embedding technique as an adjunct to our studies of membrane biosynthesis in the retina in order to test some hypotheses about cellular mechanisms of intracellular transport of opsin (29) and a large protein in ROS (30) from sites of synthesis in the RER to the region near the base of the ROS where assembly apparently occurs (16). We needed a technique which preserved structure in order to identify the intracellular components involved in opsin biosynthesis. We also wanted to test the usefulness of immunization and antibody purification using antibodies to antigens isolated from SDS polyacrylamide gels as suitable reagents for localization of antigens at the electron miroscope level. It was not obvious, before this study, that such antigenic preparations would provide antibodies that would react with aldehyde-treated membrane proteins. Our antigens, frog and cattle opsin, were adequate and localization was readily achieved. Earlier immunocytochemical studies described localization of opsin in the ROS as expected (12, 19). Jan and Revel also observed labeling with hemocyanin-conjugated anti-opsin on the plasma membrane of ROS in the scanning electron microscope (20). Our reactions along the plasma membrane (Fig. 7, *inset*) would support that conclusion in sectioned retinas.

To determine the reactivity of the anti-cattle opsin with the frog retina sections, we employed a new approach to two-stage immunocytochemistry, the biotin-avidin complex suggested by the work of Heitzmann and Richards (17), Baer et al. (2, 3), and Becker and Wilchek (5). The biotin-labeled sheep $F(ab')_2$ was readily prepared without significant interference with reactivity. Detection of the biotin-labeled antibodies with AvF was rapid and stable as predicted by its high binding constant (15). The approach provides a new and useful tool for localization since the preparation of first-stage antibodies will not be restricted by the availability of appropriate second-stage antibodies.

Both antisera to frog opsin and the antiserum to cattle opsin were prepared by comparable approaches. Immunization with the purified opsin accompanied by acrylamide and SDS leads to prompt and adequate antibody responses. Typical levels of antibody are 1.0 mg per ml in rabbits and 0.2–0.8 mg per ml in a sheep.

Each of the antibodies to frog and to cattle opsin has a different pattern of labeling of ROS when tested with the frog retina sections. All these antisera were tested after affinity purification on cattle opsin immunoabsorbents. One anti-frog opsin serum reacted comparably with both red and green ROS while the other anti-frog opsin and anti-cattle opsin antibodies reacted primarily with frog red ROS and less with frog green ROS (Fig. 7 and Table I). Prior microspectrophotometric studies have suggested differences in wavelength of maximal absorbance in these two rod photoreceptors. The red ROS absorbs light maximally at 500 nm, the green ROS at 432 nm (25). Our

[2] Papermaster, D. S., B. G. Schneider, M. Zorn, and J. P. Kraehenbuhl. Immunocytochemical localization of a large membrane protein to the incisures and margins of frog retinal rod outer segment disks. Manuscript submitted for publication.

results suggest that the spectral differences in these opsins may also be reflected in their different antigenicity although different regions of the molecules may be involved. The ultrastructural approach provided us with a unique parameter for studying this sort of heterogeneity of antigenic relationships among the opsins. Other immunochemical approaches, dependent upon the collective properties of mixed antigenic populations, could not detect the contribution of green rods which comprise <4% of the ROS mass in the frog retina (25).

The ability to distinguish red and green photoreceptors immunocytochemically also provides a new potential for analysis of photoreceptor degradation by PE cells. Disks engulfed in phagosomes still retain their distinctive antigenicity, at least at early stages of destruction (Figs. 8 and 9). Since it now appears that PE cell phagocytosis of ROS disks in mammals and frogs is triggered by diurnal cycles and light (4, 6, 24), it may be possible to test the sensitivity of various photoreceptor populations to monochromatic light exposure and assess their relative responses quantitatively by direct immunocytochemical analysis of phagosome content.

Most of the bound anti-frog opsin or anti-cattle opsin which reacts with frog red ROS is dispersed predominantly as single grains or small clusters of two to three ferritin grains. This is true for both of the ferritin-conjugated reagents, ferritin-sheep $F(ab')_2$ (Figs. 3 and 4) and AvF (Figs. 7 and 9). With anti-cattle opsin, occasional clusters of 10 or more ferritin grains are present over frog red ROS, and are more prominent over green ROS primarily because of the less dense labeling of green ROS with the anti-cattle opsin (Figs. 7 and 9). Similar clusters are also seen on both red and green ROS reacted with anti-frog opsin, but the contrast of the clustered pattern is less prominent in red ROS because of the high labeling density of dispersed molecules. The unique antigenic determinants of the different opsins may be recognized by a subset of cross-reacting antibodies in the antisera to frog and cattle opsin. Further immunochemical analysis of tissues fixed under other conditions and embedded by other techniques (32) may help in interpreting these reactions.

Similar considerations are important in assessing the variable reactions of anti-frog opsin serum with frog COS. Since the studies by Wald (33) established the homologous participation of retinaldehyde as the prosthetic group in both cone and rod photoreceptor visual pigments, attempts to establish homology of their proteins have been frustrated. One of our rabbits immunized with frog opsin responded to some determinant(s) and made antibodies which recognize an antigen in frog COS (Fig. 5 and Table I, serum no. 1). A companion rabbit immunized simultaneously with the same antigen preparation made antibodies which labeled ROS membranes and only some but not all COS. Unlabeled COS were as free of label as background regions between photoreceptor cells when reacted with this antiserum (Fig. 6 and Table I, serum no. 2). It is possible that cone proteins which constitute ~1% of frog outer segment membranes were "contaminants' in the preparation of the frog opsin immunogen. If so, this would indicate molecular homology (i.e. comparable size) since the antigen was prepared from a band excised from an SDS polyacrylamide gel. Because the rabbit anti-frog opsin sera were subsequently purified on a cattle opsin immunoabsorbent, these hypothetical antibodies to the cone protein contaminant should have been reduced proportionally by the low content of homologous cattle cone proteins present in the cattle opsin preparation used for the immunoabsorbent. Cone cells are rare in cattle retina and have much smaller outer segments than ROS (14). Alternatively, these reactions may indicate the preservation of cross-reacting antigenic determinants of opsin and the cone photopigment which are variably recognized as immunogens by some of the immunized rabbits. In some cones the photopigment may resemble opsin more than in other cones. Regardless of the alternative molecular mechanisms for explaining this observation, the reaction of rabbit anti-frog opsin with frog COS represents evidence of molecular or immunochemical homology of cone and rod photopigments. This emphasizes the phylogenetic and ontogenetic relationships of these two classes of photoreceptors.

Our results with anti-cattle opsin also indicate that the frog red rod opsin antigenic determinants more closely resemble cattle opsin than the antigens of neighboring frog green ROS. Cattle rhodopsin absorbs maximally at 500 nm and thus resembles frog red ROS rhodopsin in this aspect. Fish opsin which is the same size is also immunoprecipitated by anti-cattle opsin and anti-frog opsin (D. Papermaster, unpublished results). Jan and Revel (19) also noted cross-reactivity of rodent retina with antibody to cattle opsin. These

reactions suggest that there has been considerable conservation of opsin antigenicity over a wide range of vertebrate life.

Prior autoradiographic studies have shown a dynamic pathway of opsin biosynthesis initially involving RER and the Golgi complex (7, 8, 37). Radioactively labeled proteins migrated from these regions and were subsequently located in the mitochondrial-rich region and then at the base of the ROS (16, 36). However, it was not possible to assess by these data that the labeled proteins in the inner segment were opsin except at the final stage when some of the labeled proteins were transferred to the ROS (16). Our results confirm these autoradiographic studies and indicate that opsin antigens are associated with structures resembling Golgi complexes (Fig. 10). In the mitochondrial-rich regions and RER, the labeling density was above background levels (Table II). The high electron density of the RER and the low level of ferritin labeling make identification of membranous intermediates in opsin biosynthesis more difficult in this part of the cell. In the mitochondrial region, ferritin grains are more easily distinguished because of the low electron density of mitochondria. Autoradiographic silver grains are also seen in this area between 1 and 2 h after injection of radio-labeled amino acids in frogs (16, 37). However, the structural alteration caused by tissue dehydration does not allow us to correlate membranous structures in this region with ferritin grains. Their presence in this region at a density slightly above background does suggest, however, that intracellular channels or vesicles rather than the external plasma membrane may serve as the route for transport of opsin to the area near the base of the ROS.

We wish to thank Dr. E. R. Weibel, Anatomy Institute, University of Bern, Bern, Switzerland, for helpful discussions of morphometric analysis.

This work was supported in part by U. S. Public Health Service (U. S. P. H. S.) grants GM21714 and EY 00845, an American Cancer Society grant BC129A, the Research Center on Cellular Membranes at Yale University, and a Swiss National Science Foundation grant 3-514-0.75. D. S. Papermaster is a recipient of a U. S. P. H. S. Research Career Development Award, EY 00017 and during 1976–1977 was a Josiah Macy Jr. Faculty Scholar on leave at the Department of Chemical Immunology, Weizmann Institute of Science, Rehovot, Israel.

*Received for publication 17 June 1977, and in revised form 14 December 1977.*

## REFERENCES

1. Ainsworth, S. K., and M. J. Karnovsky. 1972. An ultrastructural staining method for enhancing the size and electron opacity of ferritin in thin sections. *J. Histochem. Cytochem.* **20**:225–229.
2. Baer, E. A., E. Skultelsky, D. Wynne, and M. Wilchek. 1976. Preparation of ferritin-avidin conjugates by reductive alkylation for use in electron microscopic cytochemistry. *J. Histochem. Cytochem.* **24**:922–939.
3. Baer, E. A., M. Wilchek, and E. Skultelsky. 1976. Affinity cytochemistry: The localization of lectin and antibody receptors on erythrocytes via the avidin biotin complex. *F. E. B. S. Lett.* **68**:240–244.
4. Basinger, S., R. Hoffman, and M. Matthes. 1976. Photoreceptor shedding is initiated by light in the frog retina. *Science (Wash. D. C.).* **194**:1074–1076.
5. Becker, J. M., and M. Wilchek. 1972. Inactivation by avidin of biotin modified bacteriophage. *Biochim. Biophys. Acta.* **264**:165–170.
6. Besharse, J. C., J. G. Hollyfield, and M. E. Rayborn. 1977. Turnover of rod photoreceptor outer segments. II. Membrane addition and loss in relation to light. *J. Cell Biol.* **75**:507–527.
7. Bok, D., S. F. Basinger, and M. O. Hall. 1974. Autoradiographic and radiobiochemical studies on the incorporation of [6-$^3$H]glucosamine into frog rhodopsin. *Exp. Eye Res.* **18**:225–240.
8. Bok, D., M. O. Hall, and P. O'Brien. 1977. The biosynthesis of rhodopsin as studied by membrane renewal in rod outer segments. *In* International Cell Biology, 1976–1977. B. R. Brinkley and K. R. Porter, editors. Rockefeller University Press, New York. 608–617.
9. Bownds, D., A. Gordon-Walker, A.-C. Gaide-Huguenin, and W. Robinson. 1971. Characterization and analysis of frog photoreceptor membranes. *J. Gen. Physiol.* **58**:225–237.
10. Cohen, A. I. 1969. Rods and cones and the problem of visual excitation. *In* The Retina. B. R. Straatsma, M. O. Hall, R. A. Allen, and F. Crescitelli, editors. University of California Press, Berkeley. 31.
11. Converse, C. A., and D. S. Papermaster. 1975. Membrane protein analysis by two-dimensional immunoelectrophoresis. *Science (Wash. D. C.).* **189**:469–472.
12. Dewey, M. M., P. K. Davis, J. K. Blasie, and L. Barr. 1969. Localization of rhodopsin antibody in the retina of the frog. *J. Mol. Biol.* **39**:395–405.
13. Elder, J. H., and D. J. Morre. 1976. Synthesis *in vitro* of intrinsic membrane proteins by free, membrane-bound and Golgi apparatus-associated polyribosomes from rat liver. *J. Biol. Chem.* **251**:5054–5068.

14. FRANK, R. N., H. D. CAVANAGH, and K. R. KENYON. 1973. Light-stimulated phosphorylation of bovine visual pigments by adenosine triphosphate. *J. Biol. Chem.* **248:**596-609.
15. GREEN, N. M. 1975. Avidin. *Adv. Protein Chem.* **29:**85-133.
16. HALL, M. O., D. BOK, and A. D. E. BACHARACH. 1969. Biosynthesis and assembly of the rod outer segment membrane system. Formation and fate of visual pigment in the frog retina. *J. Mol. Biol.* **45:**397-406.
17. HEITZMANN, H., and F. M. RICHARDS. 1974. Use of the avidin-biotin complex for specific staining of biological membranes in electron microscopy. *Proc. Natl. Acad. Sci. U. S. A.* **71:**3537-3541.
18. HIRANO, H., B. PARKHOUSE, G. L. NICOLSON, E. S. LENNOX, and S. J. SINGER. 1972. Distribution of saccharide residues on membrane fragments from a myeloma cell homogenate: its implications for membrane biogenesis. *Proc. Natl. Acad. Sci. U. S. A.* **69:**2945-2949.
19. JAN, L. Y., and J.-P. REVEL. 1974. Ultrastructural localization of rhodopsin in the vertebrate retina. *J. Cell Biol.* **62:**257-273.
20. JAN, L. Y., and J.-P. REVEL. 1975. Hemocyanin-antibody labeling of rhodopsin in mouse retina for a scanning electron microscope study. *J. Supramol. Struct.* **3:**61-66.
21. KRAEHENBUHL, J. P., and J. D. JAMIESON. 1972. Solid phase conjugation of ferritin to Fab fragments for use in antigen localization on thin sections. *Proc. Natl. Acad. Sci. U. S. A.* **69:**1771-1775.
22. KRAEHENBUHL, J. P., and J. D. JAMIESON. 1976. Enzyme labeled antibody markers for electron microscopy. *In* Methods in Immunology and Immunocytochemistry. C. A. Williams and M. W. Chase, editors. Academic Press, New York. 482-495.
23. KRAEHENBUHL, J. P., L. RACINE, and J. D. JAMIESON. 1977. Immunocytochemical localization of secretory proteins in bovine pancreatic exocrine cells. *J. Cell Biol.* **72:**406-423.
24. LAVAIL, M. M. 1976. Rod outer segment disc shedding in rat retina: relationship to cyclic lighting. *Science (Wash. D. C.).* **194:**1071-1074.
25. LIEBMAN, P. A., and G. ENTINE. 1968. Visual pigments of frog and tadpole (*Rana pipiens*). *Vision Res.* **8:**761-775.
26. MCLEAN, J. D., and S. J. SINGER. 1970. A general method for the specific staining of intracellular antigens with ferritin-antibody conjugates. *Proc. Natl. Acad. Sci. U. S. A.* **65:**122-128.
27. O'BRIEN, P. J. 1977. Differential effects of puromycin on the incorporation of precursors of rhodopsin in bovine retina. *Biochemistry.* **16:**953-958.
28. PALADE, G. 1959. Functional changes in the structure of cell components. *In* Subcellular Particles. T. Hayashi, editor. Ronald Press, New York. 64.
29. PAPERMASTER, D. S., C. A. CONVERSE, and J. SIU. 1975. Membrane biosynthesis in the frog retina: opsin transport in the photoreceptor cell. *Biochemistry.* **14:**1343-1352.
30. PAPERMASTER, D. S., C. A. CONVERSE, and M. ZORN. 1976. Biosynthetic and immunocytochemical characterization of a large protein in frog and cattle rod outer segment membranes. *Exp. Eye Res.* **23:**105-116.
31. PAPERMASTER, D. S., and W. J. DREYER. 1974. Rhodopsin content in the outer segment membranes of bovine and frog rods. *Biochemistry.* **13:**2438-2444.
32. TOKUYASU, K. T., and S. J. SINGER. 1976. Improved procedure for immunoferritin labeling of ultrathin frozen sections. *J. Cell Biol.* **71:**894-906.
33. WALD, G. 1968. Molecular basis of visual excitation. *Science (Wash. D. C.).* **162:**230-239.
34. WEIBEL, E. R., and R. P. BOLENDER. 1973. Stereological techniques for electron microscopic morphometry. *In* Principles and Techniques of Electron Microscopy. Vol. III. M. A. Hayat, editor. Van Nostrand-Reinhold, New York. 237.
35. WEIBEL, E. R., G. LOSA, and R. P. BOLENDER. 1976. Stereological method for estimating relative membrane surface area in freeze-fracture preparations of subcellular fractions. *J. Micros. (Oxf.).* **107:**255-266.
36. YOUNG, R. W. 1967. The renewal of photoreceptor cell outer segments. *J. Cell Biol.* **33:**61-72.
37. YOUNG, R. W., and B. DROZ. 1968. The renewal of protein in retinal rods and cones. *J. Cell Biol.* **39:**169-187.